

Short Papers

Dielectric Loss in Microstrip Lines

TED L. SIMPSON AND BANGJUH TSENG

Abstract—A new technique is presented for calculating dielectric loss in microstrip lines. Numerical results for several different substrates are included. These are compared with other available results and experimental data.

I. INTRODUCTION

A number of papers have been published in recent years treating losses in microstrip transmission lines [1]–[3]. But most of these efforts have been directed at the study of conductor loss. Dielectric losses are simply calculated by either empirical formulas [4], [5] or plane-wave approximation [6]. The reason behind this is, of course, for low-loss substrates, conductor loss is dominant. But in the case of monolithic MIC's, where substrates such as silicon or germanium are used, dielectric loss becomes the dominant one, and therefore has to be treated more rigorously.

In this short paper, a new method for calculating dielectric loss in microstrip is presented. This method is basically an extension of the moment method which has been used widely to calculate other microstrip characteristics such as impedances [7] and equivalent circuits of right-angled bends [8].

II. THEORY AND NUMERICAL FORMULATION

The attenuation constant due to imperfect dielectric in a medium is

$$\alpha_d = \frac{\frac{\sigma}{2} \int E^2 \cdot ds}{2P}$$

where

$$P = \frac{1}{2} \cdot \frac{V^2}{Z_0}$$

is the total power.

We may define a normalized α_d as

$$\alpha_{dn} = \frac{\alpha_d}{\sigma} = \frac{\int E^2 ds}{2V^2/Z_0}. \quad (1)$$

In (1), by assuming a voltage V across the center conductor and ground plane, the characteristic impedance Z_0 can be easily calculated by the moment method. The only problem is to evaluate the integral $\int E^2 ds$.

In applying the moment method to calculate microstrip impedance, the charge density distribution on the center conductor is obtained as an intermediate result. Once this charge density distribution is known, then the potential at a point $P(r)$ inside the dielectric can be written as

$$\Phi(r) = \int_{\text{center conductor}} G(r, r') \sigma(r') dr'. \quad (2)$$

Manuscript received June 16, 1975; revised September 12, 1975. This work was supported by the National Aeronautics and Space Administration.

The authors are with the Department of Electrical Engineering, College of Engineering, University of South Carolina, Columbia, SC 29208.

If the center conductor is divided into NW sufficiently narrow strips, then the charge density on each strip can be considered as a constant, and we can rewrite (2) as

$$\Phi(r) = \sum_{i=1}^{NW} \sigma(r_i') \int_{i\text{th strip}} G(r, r') dr'. \quad (3)$$

The integral in (3) may be expressed as

$$S\left(x, y; \frac{x_1 + x_2}{2}, H\right) = \frac{-1}{2\pi(\epsilon_0 + \epsilon)} \sum_{n=0}^{\infty} (-k)^n \cdot \left\{ B \ln \frac{(y + H_n)^2 + B^2}{(y - H_n)^2 + B^2} - A \ln \frac{(y + H_n)^2 + A^2}{(y - H_n)^2 + A^2} + 2(y + H_n) \left[\arctan \frac{B}{y + H_n} - \arctan \frac{A}{y + H_n} \right] + 2(y - H_n) \left[\arctan \frac{B}{y - H_n} - \arctan \frac{A}{y - H_n} \right] \right\} \quad (4)$$

where

$$K = \frac{\epsilon_r - 1}{\epsilon_r + 1}$$

$$H_n = (2n + 1)H$$

and

$$A = x - x_1$$

$$B = x - x_2$$

as shown in Fig. 1.

Although E can be obtained by differentiating (4), in doing so, more terms will be generated in the infinite series, and this increases the computing time considerably. Therefore, it is computed numerically as follows.

The total integration area over which the integral in (1) is to be carried out is divided into $2M \times 2N$ subareas ($\Delta X \cdot \Delta Y$), and the potential at every corner of each subarea is calculated. We then define two vectors, U and V as depicted in Fig. 2. The vector normal to both U and V is

$$N = U \times V = N_x \hat{a}_x + N_y \hat{a}_y + N_z \hat{a}_z$$

and $|E|^2$ is simply (see Appendix I)

$$E^2 = \frac{N_x^2 + N_y^2}{N_z^2}. \quad (5)$$

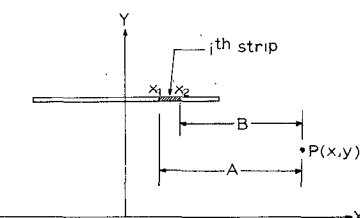
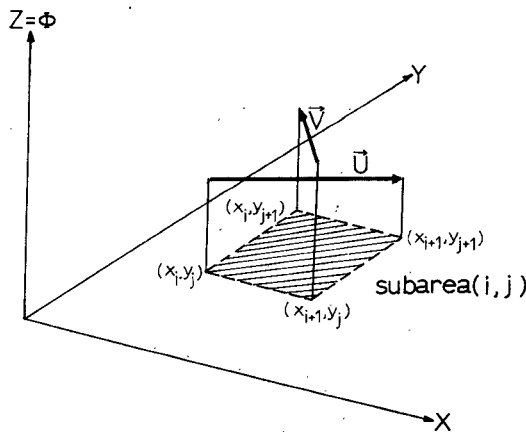


Fig. 1. Definition of variables A and B in (4).

Fig. 2. Definition of vectors U and V .

The integral in (1) simply becomes

$$\int E^2 ds = \sum_{i=1}^M \sum_{j=1}^N (E_{ij}^2) \Delta X \Delta Y.$$

III. NUMERICAL RESULTS

A computer program was written to carry out the numerical integration. After some investigations, the parameters NW , M , N , ΔW , ΔX , and ΔY (as shown in Fig. 3) were chosen under the following criteria:

$$NW = 20, \quad W/H \leq 1$$

$$NW = 20 + 5(W/H - 1), \quad W/H > 1 \quad (6a)$$

$$N = H/W \cdot NW \quad (6b)$$

$$M = \frac{NW}{2} + K \cdot \frac{H}{W} \cdot NW \quad (6c)$$

where

$$K = 2.7 - 0.1\epsilon_r$$

$$\Delta W = \Delta X \simeq \Delta Y. \quad (6d)$$

It is worthwhile to point out that parameter K in condition 6(c) which defines the total integration area for a specified NW , is empirically chosen such that the summation of E^2 outside the inte-

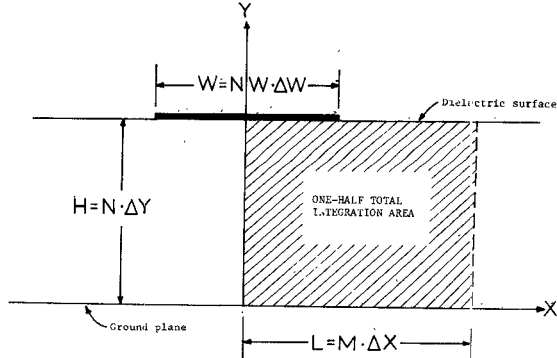


Fig. 3. Parameters involved in numerical integration.

gration area is less than one percent of that inside this area for $w/H \geq 0.4$. The errors of results calculated under these conditions are estimated to be less than -2.5 percent (as compared to that of finer subdivision and larger total integration area) for $0.4 \leq W/H \leq 6.0$ and $2 \leq \epsilon_r \leq 11.7$. The computer results obtained by this method for several different dielectric constants are compared with another theory [4] in Table I. The calculated attenuation constant of a microstrip line on silicon substrate ($\epsilon_r = 11.7$) is also compared with the experimental data from Hyltin [9] in Fig. 4.

These numerical calculations were carried out by an IBM 360/75 computer. The computing time for each structure was less than 5 s. A Fortran source listing of this program is available by request from the authors.

APPENDIX

Derivation of (5): Assuming that each subarea is sufficiently small that $\Phi(x, y)$ can be approximated locally by its tangent plane, then we can write

$$\Phi(x, y) = z(x, y) \simeq dx + dy + c.$$

In vector notation, a plane with a normal vector N can be represented by the equation

$$(\mathbf{R} - \mathbf{P}) \cdot \mathbf{N} = 0$$

where

$$\mathbf{R} = x\hat{a}_x + y\hat{a}_y + z\hat{a}_z$$

$$\mathbf{P} = x_1\hat{a}_x + y_1\hat{a}_y + z_1\hat{a}_z$$

TABLE I
NORMALIZED ATTENUATION CONSTANTS OF MICROSTRIP LINES

W/H	$\epsilon_r = 2.22$		$\epsilon_r = 3.82$		$\epsilon_r = 9.0$		$\epsilon_r = 11.7$	
	α_{dn}^a	α_{dn}^b	α_{dn}^a	α_{dn}^b	α_{dn}^a	α_{dn}^b	α_{dn}^a	α_{dn}^b
0.4	743.95	743.80	596.94	594.56	406.81	405.03	359.69	357.60
0.6	764.34	760.20	611.13	606.02	415.07	411.89	366.76	363.51
0.8	780.85	774.70	622.59	616.18	421.73	417.97	372.46	368.72
1.0	794.87	787.91	632.28	625.48	427.36	423.44	377.27	373.67
2.0	844.86	836.81	666.67	659.53	447.27	443.33	394.55	390.87
3.0	877.81	871.21	689.18	683.59	460.28	457.49	405.45	402.94
4.0	902.12	896.40	705.71	700.79	469.82	467.31	413.62	411.54
5.0	921.10	916.37	718.58	714.34	477.24	475.12	419.97	418.14
6.0	936.47	931.14	728.97	724.67	483.23	481.12	425.10	423.36

Note: α_{dn} in decibel ohms.

^a Results obtained by Schneider's theory [4].

^b Results obtained by numerical integration.

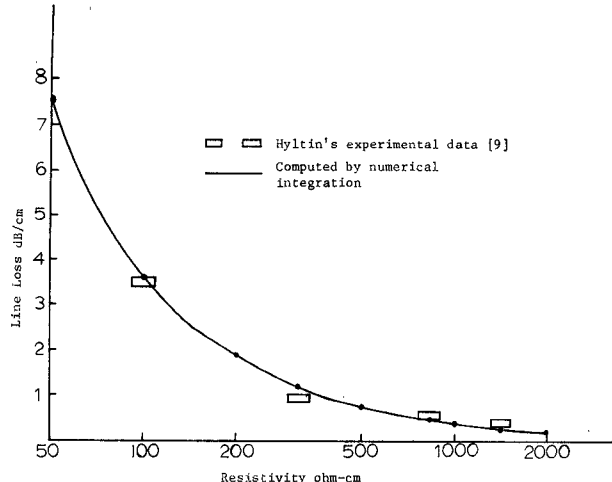


Fig. 4. Microstrip line loss versus resistivity of the dielectric substrates.

 $\epsilon_r = 11.7$.the point (x_1, y_1, z_1) is on this plane.

Let

$$P \cdot N = C_1.$$

Then

$$R \cdot N = C_1$$

or

$$xN_x + yN_y + zN_z = C_1$$

$$z(x, y) = \Phi(x, y) = \frac{C_1 - xN_x - yN_y}{N_z}$$

$$E = -\frac{\partial \Phi}{\partial x} \hat{a}_x - \frac{\partial \Phi}{\partial y} \hat{a}_y$$

$$= \frac{N_x}{N_z} \hat{a}_x + \frac{N_y}{N_z} \hat{a}_y$$

$$|E|^2 = \frac{N_x^2 + N_y^2}{N_z^2}.$$

REFERENCES

- [1] R. A. Pucell, D. J. Massé, and C. P. Hartwig, "Losses in microstrip," *IEEE Trans. Microwave Theory Tech.*, vol. MTT-16, pp. 342-350, June 1968.
- [2] M. V. Schneider, "Microstrip lines for microwave integrated circuits," *Bell Syst. Tech. J.*, vol. 48, pp. 1421-1444, May-June 1969.
- [3] R. Horton, B. Easter, and A. Gopinath, "Variation of microstrip losses with thickness of strip," *Electron. Lett.*, vol. 7, pp. 490-491, Aug. 26, 1971.
- [4] M. V. Schneider, "Dielectric loss in integrated microwave circuits," *Bell Syst. Tech. J.*, vol. 48, pp. 2325-2332, Sept. 1969.
- [5] J. D. Welch and H. J. Pratt, "Losses in microstrip transmission systems for integrated microwave circuits," *NEREM Rec.*, vol. 8, pp. 100-101, Nov. 1966.
- [6] M. Caulton, J. J. Hughes, and H. Sobol, "Measurement of the properties of microstrip transmission lines for microwave integrated circuits," *RCA Rev.*, vol. 27, pp. 377-391, Sept. 1966.
- [7] A. Farrar and A. T. Adams, "Characteristic impedance of microstrip by the method of moments," *IEEE Trans. Microwave Theory Tech.*, (Corresp.), vol. MTT-18, pp. 65-66, Jan. 1970.
- [8] A. Gopinath and B. Easter, "Moment method of calculating discontinuity inductance of microstrip right-angled bends," *IEEE Trans. Microwave Theory Tech. (Short Papers)*, vol. MTT-22, pp. 880-883, Oct. 1974.
- [9] T. M. Hyltin, "Microstrip transmission on semiconductor dielectrics," *IEEE Trans. Microwave Theory Tech. (1965 Symposium Issue)*, vol. MTT-13, pp. 777-781, Nov. 1965.

The Electric-Dipole Resonances of Ring Resonators of Very High Permittivity

M. VERPLANKEN AND J. VAN BLADEL, FELLOW, IEEE

Abstract—The lowest confined mode in a coaxial ring resonator is investigated. Data are given about the Q of the mode, the eigen-electric dipole at resonance, and the structure of the electric field surrounding the resonator. The data are valid for high, but finite values of ϵ_r .

I. INTRODUCTION

In a previous paper [1], Van Bladel has shown that a dielectric body of revolution [Fig. 1(a)] admits, in the limit $\epsilon_r = N^2 \rightarrow \infty$, a resonant mode of the form

$$\bar{H}_m = \beta_m(r, z) \bar{u}_\phi \quad (1)$$

where β_m satisfies

$$\frac{\partial^2 \beta_m}{\partial r^2} + \frac{1}{r} \frac{\partial \beta_m}{\partial r} + \frac{\partial^2 \beta_m}{\partial z^2} - \frac{\beta_m}{r^2} + k_m^2 \beta_m = 0 \quad \text{in } S. \quad (2)$$

In addition, β_m vanishes on the outer contour (c) and on the z axis. The mode under discussion is a *confined mode*, which means that it takes the value (1) in the dielectric, but vanishes outside S . For such a case the boundary surface acts as a magnetic wall. When N is finite but large, the mode is found to radiate like an electric dipole of moment \bar{p}_e . As a result, energy is lost by radiation, and a finite Q affects the resonance. The value of Q is proportional with N^5 , while it is proportional with N^3 for a magnetic-dipole mode. The strong increase of Q with N is the reason why the electric-dipole mode is of interest for applications. We proceed to calculate \bar{p}_e and Q for the ring resonator shown in Fig. 1(b). The limit form $b = 0$ corresponds to a circular cylinder, a structure which is often used in practice.

II. FORMULAS FOR DIPOLE MOMENT AND Q

The determination of these quantities requires solution of the following exterior potential problem [1]

$$\nabla^2 \phi = 0 \quad \text{outside } S$$

Manuscript received April 14, 1975, revised July 14, 1975.

The authors are with the Laboratory for Electromagnetism and Acoustics, University of Ghent, B-900 Ghent, Belgium.